

Electronic Supporting Information

Chemically coded time-programmed self-assembly

*Eszter Tóth-Szeles^a, Judit Horváth^b, Gábor Holló^{a,c}, Rózsa Szűcs^a, Hideyuki Nakanishi^c,
István Lagzi^{a,c*}*

^a Department of Physics, Budapest University of Technology and Economics, 1111, Budafoki út 8, Budapest, Hungary

^b Institute of Chemistry, Eötvös Loránd University, P. O. Box, H-1518 112, Hungary

^c Department of Macromolecular Science and Engineering, Graduate School of Science and Technology, Kyoto Institute of Technology, Matsugasaki, Kyoto 606-8585, Japan

Synthesis of the pH-responsive gel filaments:

The chemicals

- *N*-isopropylacrylamide (NIPA, Aldrich, 97%),
- *N*-*tert* butylacrylamide (NTBA, Acros),
- *N*-[3-(dimethylamino)propyl]methacrylamide (DMAPrMAA, Aldrich, 99%),
- *N,N'*-methylenebisacrylamide (Bis, Fluka, purum),
- *N,N,N',N'*-tetramethylethylenediamine (TEMED, Amiresco, ultra pure),
- sodium sulfite (BDH Prolabo, Reag.Ph.Eur.),
- potassium persulfate (KPS, Reachim)

were used as received.

The pH-responsiveness of the gel was provided by tertiary amine functional groups¹ (3.00% *n/n* of the monomers). In order to have a large enough swelling-shrinking response at room temperature, the more hydrophobic monomer NTBA was added to NIPA in 20% *n/n*.

The polymer network of the gels was synthesized by free-radical crosslinking copolymerization initiated either by TEMED/KPS or by sodium sulfite/KPS redox couple. As solvent, *tert*-butanol/water mixtures of the ratios from 8:4 to 6:4 (v/v) were used.

The thin gel cylinders for the kinetics and equilibrium swelling tests described below were synthesized in glass capillaries of 1.50 mm inner diameter. The gel filaments used with the time-programme had an initial diameter of 1.00 mm at the synthesis.

The gel cylinders were first washed in 2:1 and 3:2 ethanol/water mixtures. To get temporally rigid filaments that can be cut, manipulated, and glued to a support, the filaments were collapsed by a rapid change of the solvent to aqueous 0.5 M ammonium acetate solution. For details see our previous works.²⁻⁴

Shrinking and swelling kinetics – The role of the solvent composition during polymerization

The rate of swelling and shrinking of gels is limited by the transport of the swelling medium and the collective motion of the network chains. This sets a limit to their use as on-off switches. Higher rates can be obtained by microstructured (macroporous) gels that contain denser and looser regions on the microscale. They behave like a sponge and expel water relatively unhindered from their inner core through their pore system. These gels can be, *e.g.*, scaffolds of lightly crosslinked microgels⁵ or, simpler, so called microphase-separated porous structured gels. To obtain such gels, microphase separation should occur during the polymerization, so that dense domains of aggregates are fixed by crosslinking and loosely connected by several longer network chains.^{6,7} These latter chains ensure an excellent elasticity up to high degrees of deformation without rupture.

We got microphase-separated porous structured gels (at the same time keeping the appropriate pH-response) by tuning the solvent composition for the crosslinking polymerization (Table S1).

The microstructure of the resulting polymer network depends sensitively on the solvent composition.^{8,9} In a so called “good solvent” (2:1 BuOH/water ratio) the forming chains are expanded, well-solvated, the gel is transparent (clear), and the network is homogeneous (gel A). The quality of the solvent rapidly decreases by increasing the ratio of water in this intermediate composition range, therefore the forming gel is translucent in 7:4 BuOH/water (gel B) and opaque in 3:2 BuOH/water (gel C). In the course of polymerization, the initially clear reaction mixture gradually turns turbid after about 15 min due to the appearance and aggregation of insufficiently solvated, shrunken polymer chains. A porous structure from these heterogeneities forms.

An accompanying consequence of using a less good solvent is the slight syneresis of gels B and C during the polymerization (the gel volume is somewhat lower than that of the pregel solution). Therefore, gels B and C detach from the glass capillary wall after synthesis and can be easily removed (pulled out).

Table S1 Molar amounts in 11.0 mL solvent mixture

Gel composition:	A	B	C “fast gel”
<i>tert</i> -butanol/water (v/v)	2:1 (≡ 8:4)	7:4	3:2 (≡ 6:4)
NTBA	2.000 mmol	2.000 mmol	2.000 mmol
NIPA	8.000 mmol	8.000 mmol	8.000 mmol
Bis	0.050 mmol	0.050 mmol	0.050 mmol
DMAPrMAAm	0.315 mmol	0.315 mmol	0.315 mmol
TEMED	0.200 mmol	0.200 mmol	0.200 mmol
Na ₂ SO ₃	-	-	-
KPS	0.100 mmol	0.100 mmol	0.100 mmol

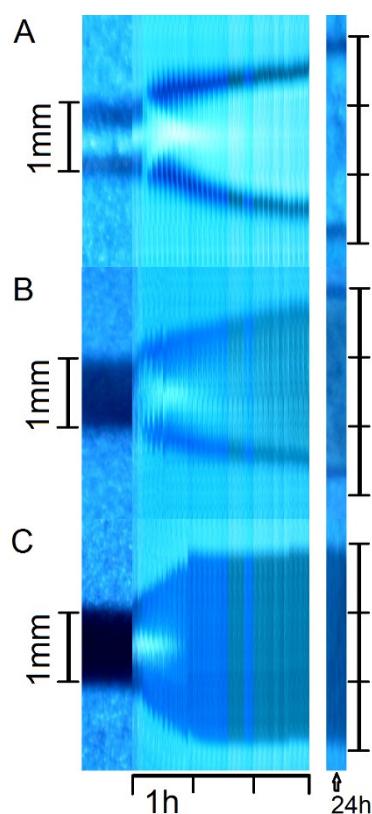


Figure S1 Kinetics of swelling after a temperature drop of the surrounding buffer solution from 32.0 °C to 23.0 °C at constant pH 8.36. For the solvent composition at the synthesis of gels A, B, and C refer to Table S1. *N.B.*: The “fast gel” remains turbid even swollen.

Swelling kinetics measurements (Fig. S1) reveal a striking difference between gel C (“fast gel”) and A and B (“normal” gels). Swelling equilibrium of the “fast gel” C (from 0.95 mm to 2.70 mm) is reached in 55–60 min. For comparison, the normal network gel A swells only to 66% of its final diameter in 1 hour and to 80% in 3 hours (finally the fully swollen 2.70 mm diameter is reached in 24 h).

The opposite process (not shown), the shrinking of the “fast gel” C (from 2.45 mm to 1.00 mm, so to 40% of the swollen diameter) is complete in 10 minutes. During the same time, the normal gel A shrinks from 2.45 mm to only 2.20 mm, so it still has 90% of its initial diameter (and still 81% after 20 min).

Swelling of the porous gel is facilitated by the fact that water can penetrate inside the collapsed gel through the pore system thus the contact area with water is higher than in a conventional gel. At the same time, swelling remains much slower than the collapse which is a general observation in pNIPA-based gels. Supposedly, the hydrophobic interaction between the isopropyl functions in the collapsed state is difficult to break during the hydration process.⁶

Sharpness of the swelling/shrinking transition as a function of pH – The role of the reducing agent in the initiation process

TEMED is a commonly used component with persulfates for initiating free-radical polymerization in aqueous solution. At the same time, we want to use a comonomer with a weak base function (DMAPrMAA) in order to get a pH-responsive gel in the moderately basic region, around between pH 8–9. *N.B.*, DMAPrMAA and TEMED are both tertiary amines, and they might be present in a comparable amount in the network (Table S2, gel D) because TEMED radicals are incorporated at chain start or termination.

Table S2 Molar amounts in 11.0 mL solvent mixture

Gel composition:	D	E
<i>tert</i> -butanol/water (v/v)	8:5 (\equiv 6,5:4)	3:2 (\equiv 6:4)
NTBA	2.000 mmol	2.000 mmol
NIPA	8.000 mmol	8.000 mmol
Bis	0.050 mmol	0.033 mmol
DMAPrMAAm	0.315 mmol	0.315 mmol
TEMED	0.200 mmol	-
Na₂SO₃	-	0.164 mmol
KPS	0.100 mmol	0.075 mmol

DMAPrMAA gels initiated by TEMED (D in Table S2) did not give a same sharp pH-response (that is, within 1–1.5 pH units) that we had got in our previous works for gels operational in different pH-regions below pH 7. Even by optimizing the temperature to get a maximal size-change, the transition of the gel of composition D from swollen to shrunken spread over more than 2 pH units (Figure S2). This finding confirms that functions of somewhat different base strengths are present in the network, *that is*, amine functions on TEMED and the DMAPrMAA comonomer are not identical and have the consequence of a pK_b distribution.

However, this problem was overcome by omitting TEMED and using the inorganic sulfite ion as reducing agent (gel E in Table S2). This necessary change together with a slight adjustment of the amount of the crosslinker resulted in a sharp swollen to shrunken transition, that is to 38% of the initial diameter, within 1.25 pH units (from pH 8.00 to 9.25).

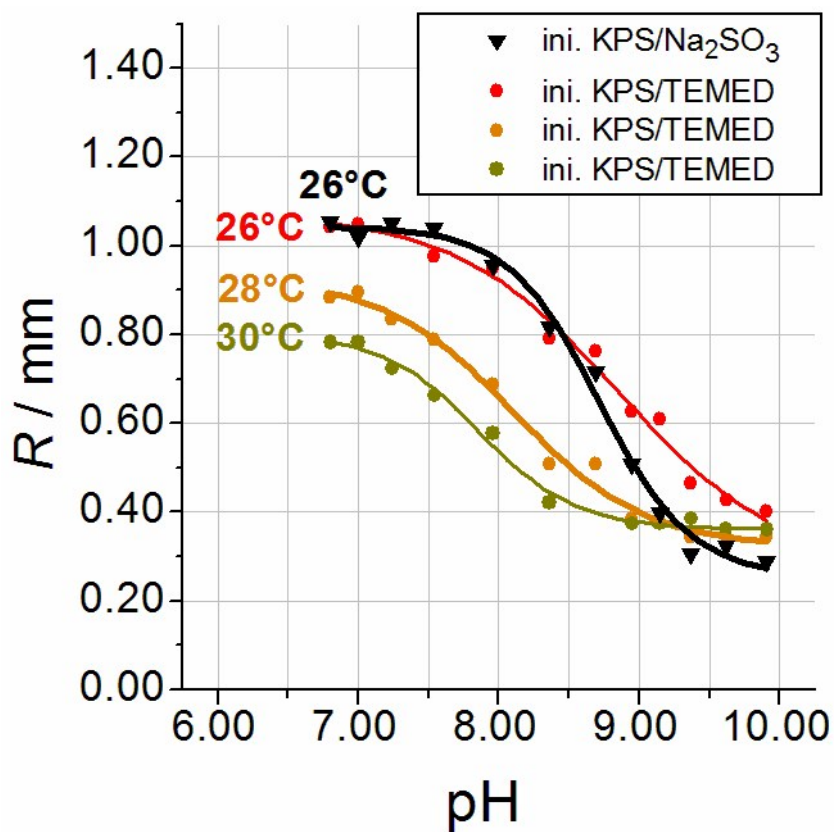


Figure S2 Radius of the cylindrical gels ($R_0 = 0.750$ mm at synthesis) in swelling equilibrium in Britton–Robinson buffers with $[\text{Na}^+]_{\text{tot}} = 50$ mM. For gel compositions see Table S2.

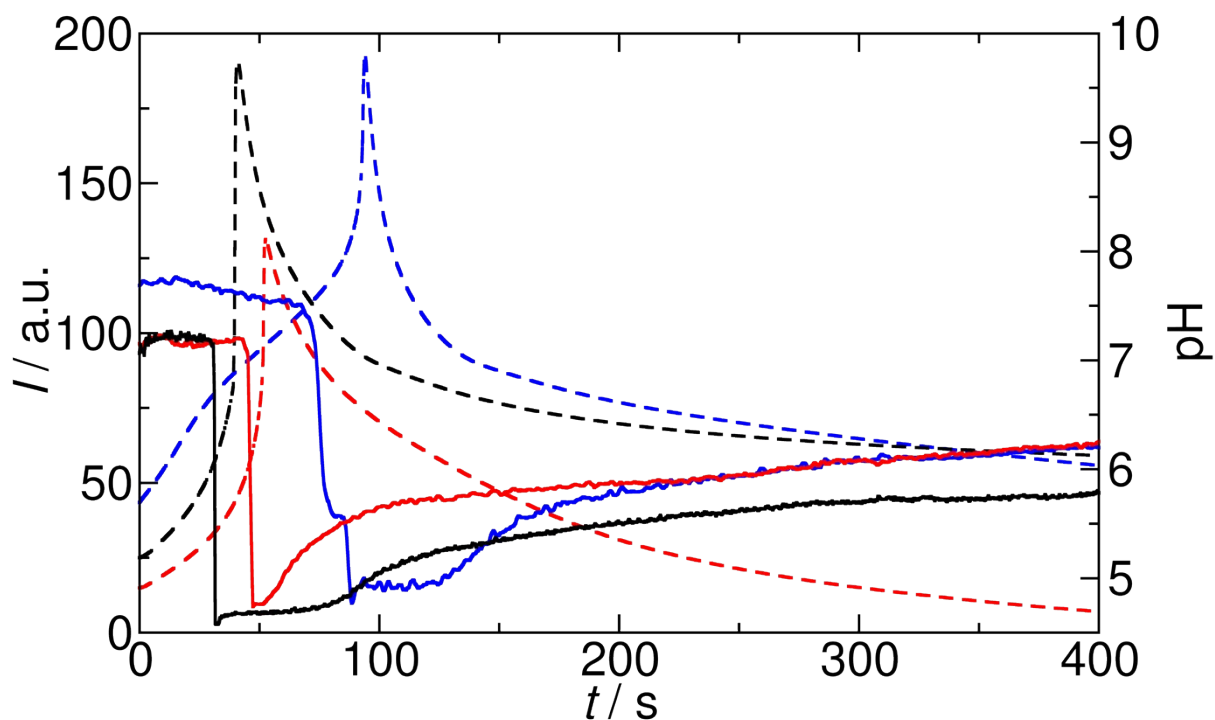


Figure S3 The internally programmed time course of pH (dashed lines) and scattered light intensity (grayscale) (solid lines) from the vesicles during the vesicle-micelle-vesicle rearrangement in the MGS and GL + oleic acid system at different initial reactant concentrations. Black: $[\text{CH}_2(\text{OH})_2]_0 = 0.2000 \text{ M}$, $[\text{GL}]_0 = 0.0100 \text{ M}$, Red: $[\text{CH}_2(\text{OH})_2]_0 = 0.2000 \text{ M}$, $[\text{GL}]_0 = 0.0040 \text{ M}$, Blue: $[\text{CH}_2(\text{OH})_2]_0 = 0.1125 \text{ M}$, $[\text{GL}]_0 = 0.0100 \text{ M}$. The fixed initial concentrations were $[\text{SO}_3^{2-}]_0 = 0.0050 \text{ M}$, $[\text{HSO}_3^-]_0 = 0.0500 \text{ M}$ and $[\text{OA}] = 0.00125 \text{ M}$.

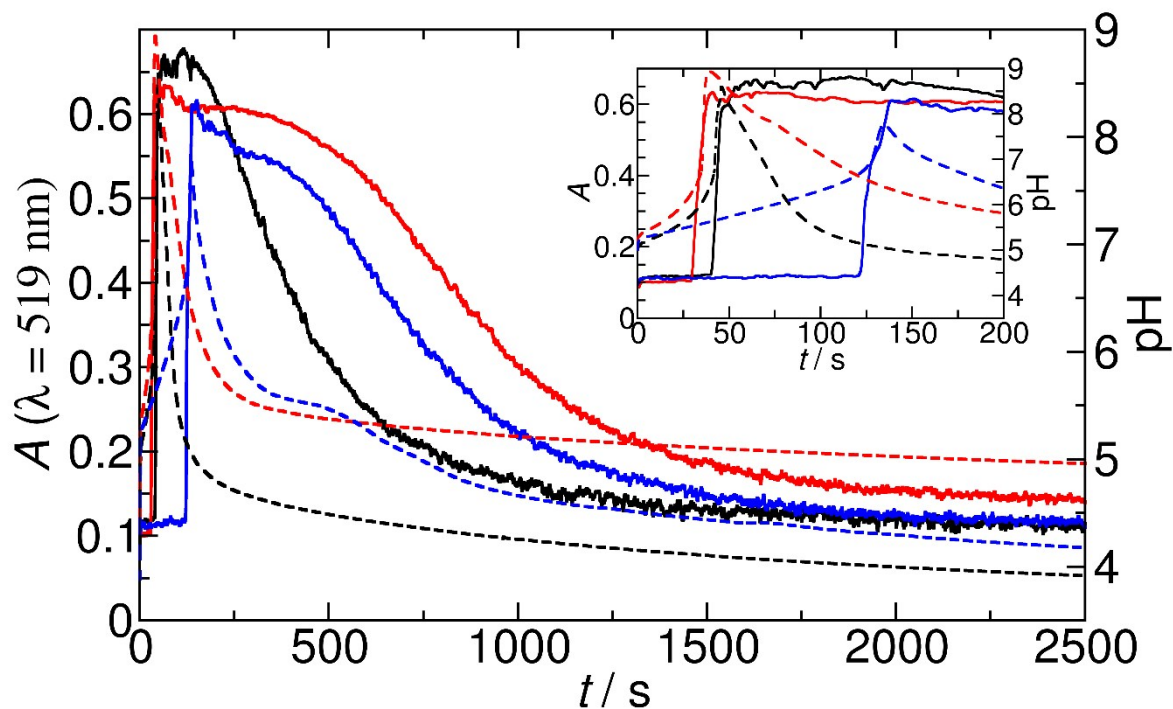


Figure S4 The internally programmed time course of pH (dashed lines) and absorbance (solid lines) resulting from the surface plasmon resonance of the free (non-aggregated) fraction of the AuNP-s in the MGS and GL + AuNP system at different initial reactant concentrations. Black: $[\text{CH}_2(\text{OH})_2]_0 = 0.2000 \text{ M}$, $[\text{GL}]_0 = 0.0100 \text{ M}$, Red: $[\text{CH}_2(\text{OH})_2]_0 = 0.2000 \text{ M}$, $[\text{GL}]_0 = 0.0040 \text{ M}$, Blue: $[\text{CH}_2(\text{OH})_2]_0 = 0.1125 \text{ M}$, $[\text{GL}]_0 = 0.0100 \text{ M}$. The fixed initial concentrations were $[\text{SO}_3^{2-}]_0 = 0.0050 \text{ M}$, $[\text{HSO}_3^-]_0 = 0.0500 \text{ M}$ and the concentration of the carboxyl group attached to the nanoparticles ($\text{COOH}@\text{AuNP}$) was $3.53 \times 10^{-5} \text{ M}$.

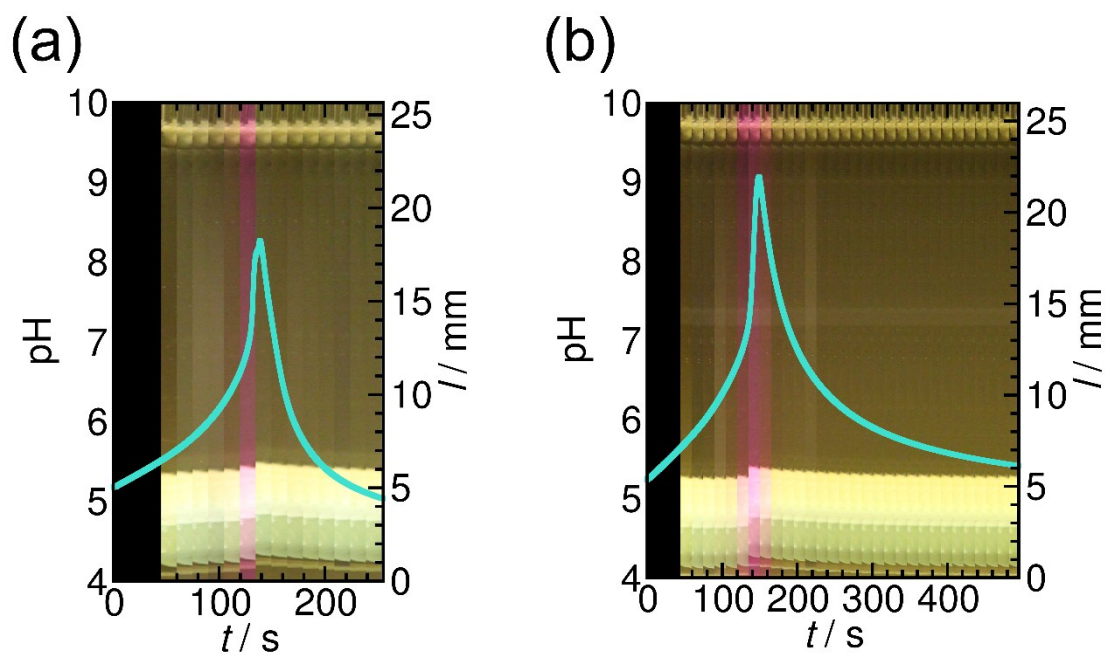
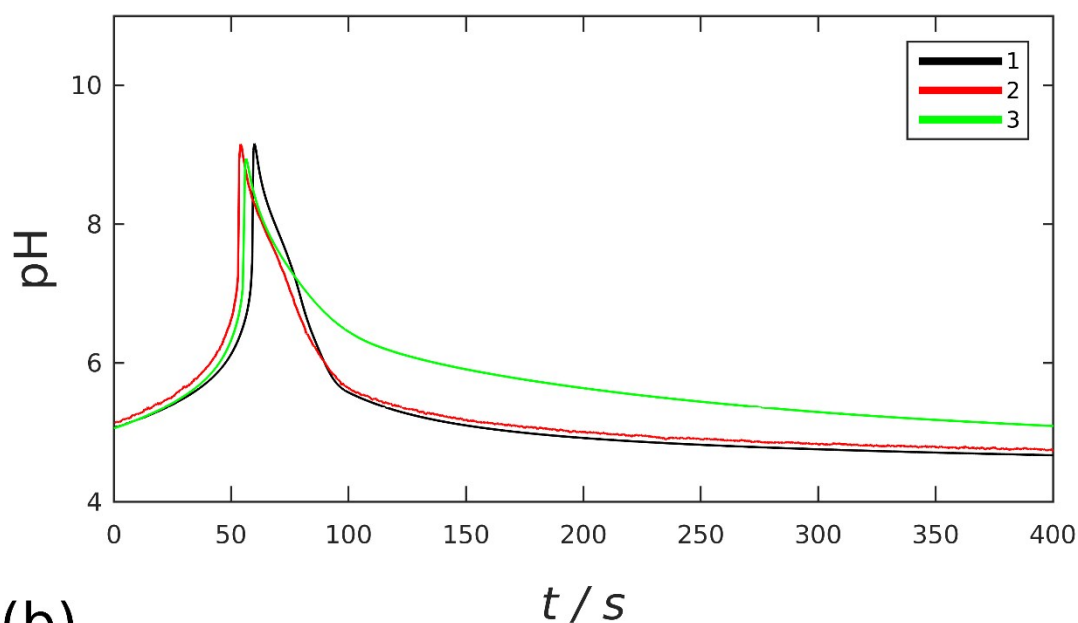


Figure S5 Space-time plots of the gel length and the synchronous pH-change (blue line) in the MGS and GL system at various lactone concentration. (a): $[GL]_0 = 0.0100$ M and (b): $[GL]_0 = 0.0040$ M. Fixed parameters: $[Phenol\ Red]_0 = 0.0145$ mM, $[CH_2(OH)_2]_0 = 0.1125$ M, $[SO_3^{2-}]_0 = 0.0050$ M, $[HSO_3^-]_0 = 0.0500$ M. The system was unstirred and $\theta = 25 \pm 0.5$ °C.

The MGS and GL system provides short and symmetric t_{tr} -s which are shorter than 50 s, that is, shorter than the characteristic diffusion time of hydroxide ions (promoters in the time programme) between the surface and the core of the 0.75 mm diameter cylindrical gel filament. The asymmetry between the rate of shrinking and reswelling (described above) can be clearly observed (Fig. S5b) even in spite of the rather small variation in length. The size-response could be greatly enhanced by using finer filaments (with diameter on the micrometer-scale), separately or in a bunch.¹⁰

(a)



(b)

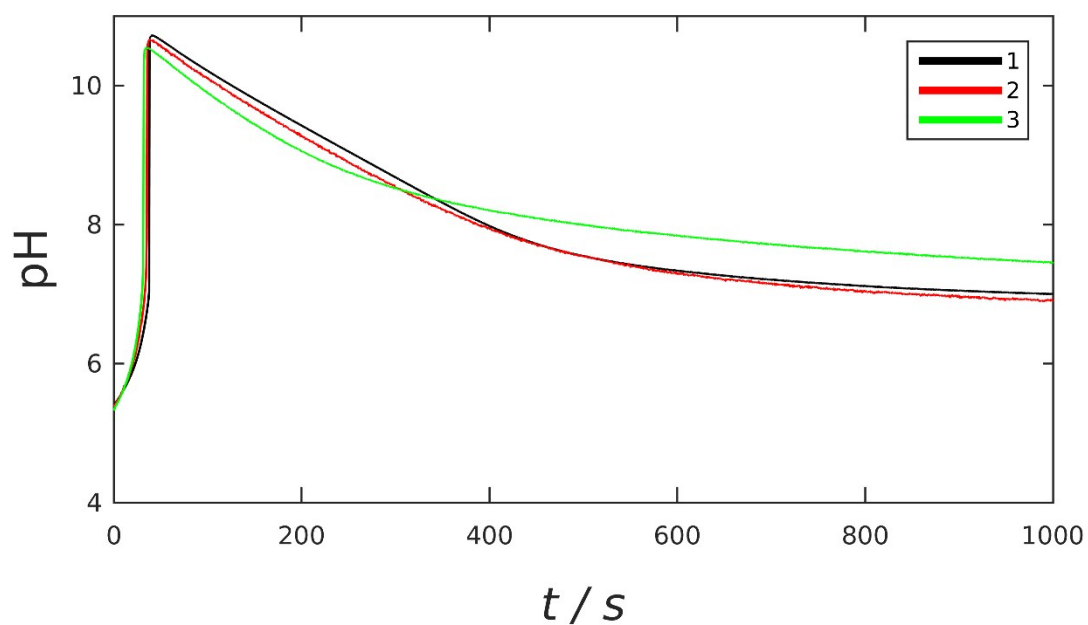


Figure S6 The pH – time curves in the presence of AuNPs in the MGS and GL (a) and MGS and VL (b) systems with the fixed initial concentrations: $[\text{CH}_2(\text{OH})_2]_0 = 0.2000 \text{ M}$, $[\text{SO}_3^{2-}]_0 = 0.0050 \text{ M}$, $[\text{HSO}_3^-]_0 = 0.0500 \text{ M}$, (a): $[\text{GL}]_0 = 0.0100 \text{ M}$, (b): $[\text{VL}]_0 = 0.0100 \text{ M}$. Black, red and green lines correspond to $[\text{COOH@AuNP}]_0 = 0 \text{ M}$, $[\text{COOH@AuNP}]_0 = 0.00003 \text{ M}$, $[\text{COOH@AuNP}]_0 = 0.00050 \text{ M}$, respectively.

Table S3 The mechanism of the system with gluconolactone and oleic acid. The rate constants (R1-R10) were taken from the literature ¹¹, and we estimated the rate constants of the oleic acid protonation (R11) with a 8.5 pKa value. The set of ordinary differential equations was integrated in time with a forward Euler method with an appropriate initial condition used in experiments.

	Reaction	Rate constants
(R1)	$CH_2(OH)_2 \rightleftharpoons CH_2O + H_2O$	$k_1 = 5.5 \times 10^{-3} \text{ s}^{-1}$
		$k_{OH} = 500 \text{ M}^{-1}\text{s}^{-1}$
		$k_{-1} = 10 \text{ s}^{-1}$
(R2)	$HSO_3^- \rightleftharpoons SO_3^{2-} + H^+$	$k_2 = 3.1 \times 10^3 \text{ s}^{-1}$
		$k_{-2} = 5 \times 10^{10} \text{ M}^{-1}\text{s}^{-1}$
(R3)	$CH_2O + SO_3^{2-} \rightarrow CH_2(O^-)SO_3^-$	$k_3 = 5.4 \times 10^6 \text{ M}^{-1}\text{s}^{-1}$
(R4)	$CH_2(O^-)SO_3^- + H^+ \rightleftharpoons CH_2(OH)SO_3^-$	$k_4 = 1 \times 10^{10} \text{ M}^{-1}\text{s}^{-1}$
		$k_{-4} = 2 \times 10^{-3} \text{ s}^{-1}$
(R5)	$H_2O \rightleftharpoons H^+ + OH^-$	$k_5 = 1 \times 10^{-3} \text{ Ms}^{-1}$
		$k_{-5} = 1 \times 10^{11} \text{ M}^{-1}\text{s}^{-1}$
(R6)	$CH_2O + HSO_3^- \rightarrow CH_2(OH)SO_3^-$	$k_6 = 4.5 \times 10^2 \text{ M}^{-1}\text{s}^{-1}$
(R7)	$CH_2(OH)_2 + SO_3^{2-} \rightarrow CH_2(O^-)SO_3^- + H_2O$	$k_7 = 1.2 \text{ M}^{-1}\text{s}^{-1}$
(R8)	$CH_2(OH)_2 + HSO_3^- \rightarrow CH_2(OH)SO_3^- + H_2O$	$k_8 = 0.1 \text{ M}^{-1}\text{s}^{-1}$
(R9)	$GL + H_2O \rightarrow GA$	$k_9 = 1 \times 10^{-4} \text{ s}^{-1}$
		$k_{OH} = 4 \times 10^3 \text{ M}^{-1}\text{s}^{-1}$
		$k_{-9} = 2 \times 10^{-5} \text{ s}^{-1}$
(R10)	$GA \rightleftharpoons GA^- + H^+$	$k_{10} = 2.5 \times 10^2 \text{ s}^{-1}$
		$k_{-10} = 1 \times 10^6 \text{ M}^{-1}\text{s}^{-1}$
(R11)	$OA \rightleftharpoons OA^- + H^+$	$k_{11} = 12.6491 \text{ s}^{-1}$
		$k_{-11} = 4 \times 10^9 \text{ M}^{-1}\text{s}^{-1}$

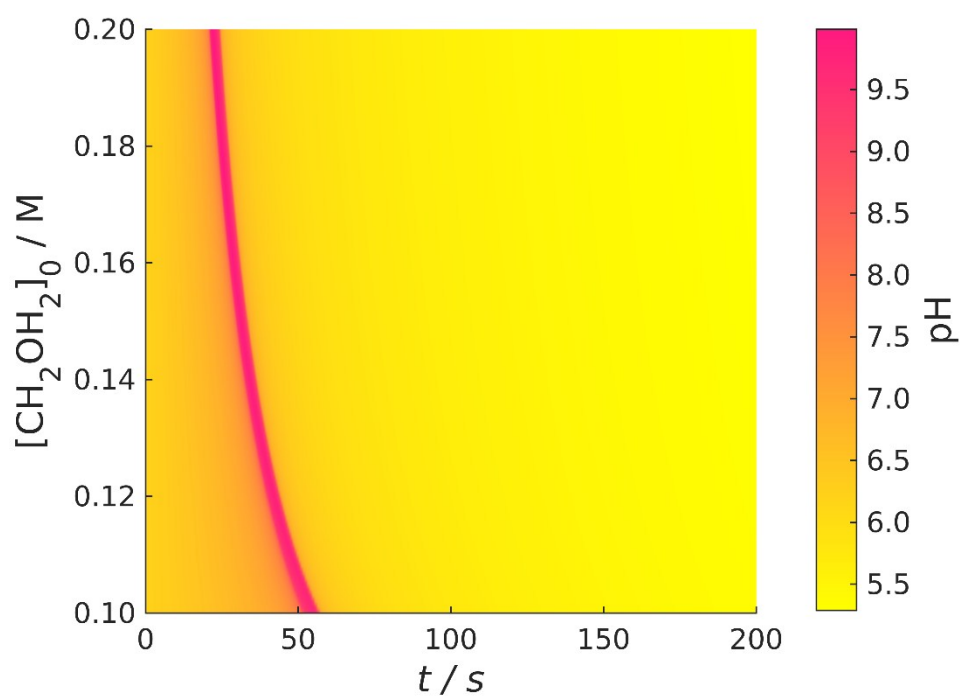
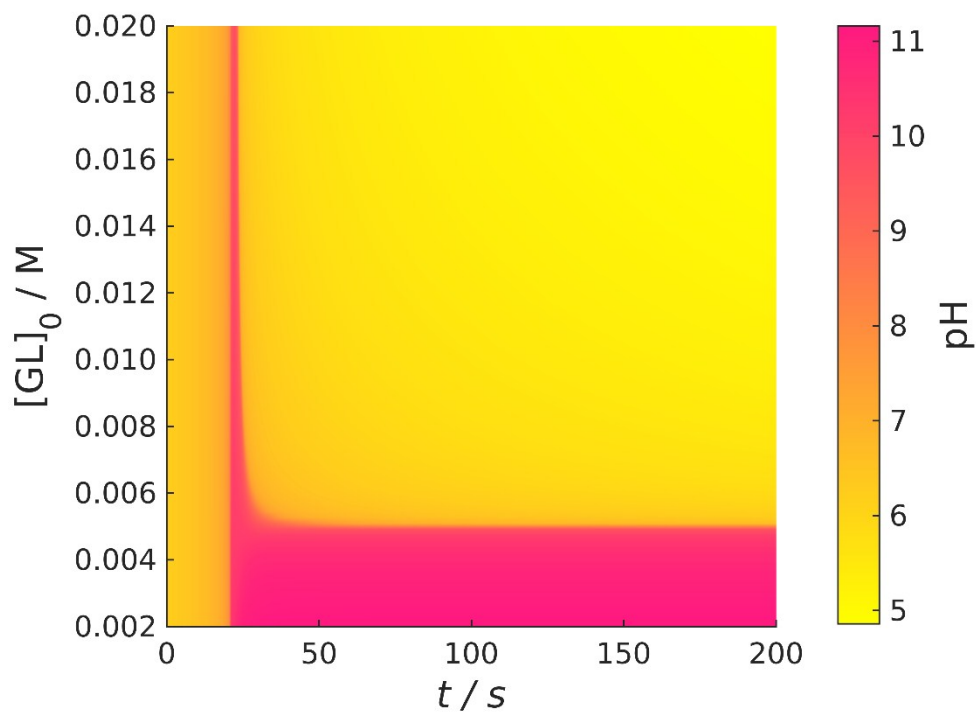


Figure S7 The calculated pH – time curves. The fixed initial concentrations: $[\text{GL}]_0 = 0.0100$ M, $[\text{SO}_3^{2-}]_0 = 0.005$ M, $[\text{HSO}_3^-]_0 = 0.0500$ M and we changed $[\text{CH}_2(\text{OH})_2]_0$ from 0.1000 M to



0.2000 M.

Figure S8 The calculated pH – time curves. The fixed initial concentrations: $[\text{CH}_2(\text{OH})_2]_0 = 0.2000 \text{ M}$, $[\text{SO}_3^{2-}]_0 = 0.0050 \text{ M}$, $[\text{HSO}_3^-]_0 = 0.0500 \text{ M}$ and we changed $[\text{GL}]_0$ from 0.0020 M to 0.0200 M .

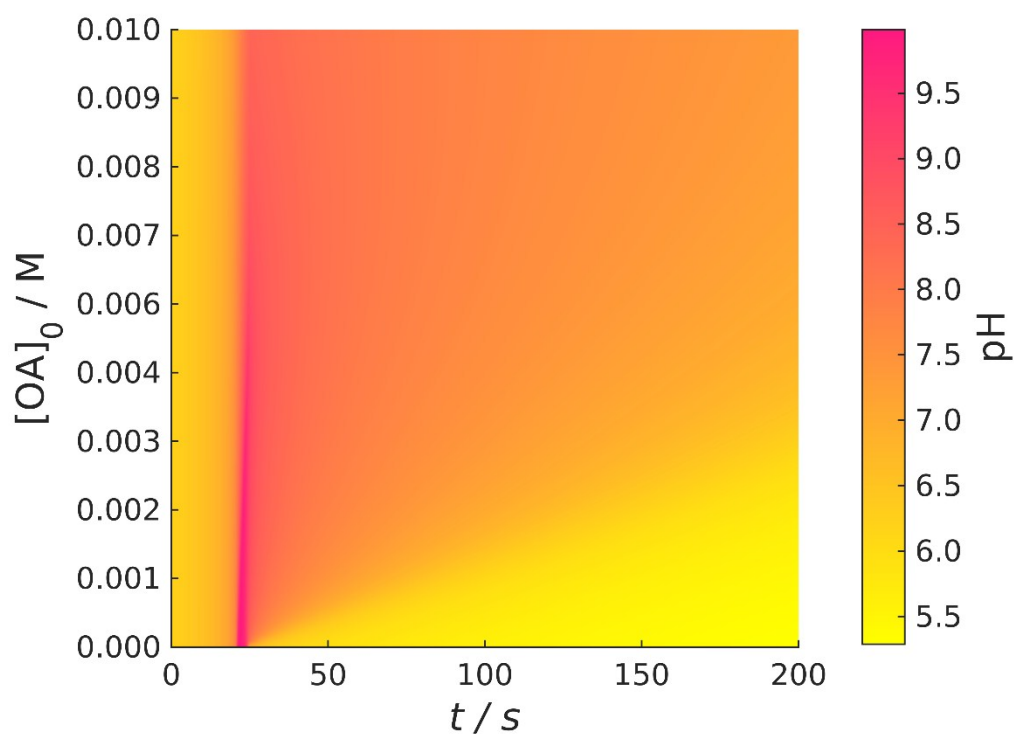


Figure S9 The calculated pH – time curves. The fixed initial concentrations: $[\text{CH}_2(\text{OH})_2]_0 = 0.2000 \text{ M}$, $[\text{GL}]_0 = 0.0100 \text{ M}$, $[\text{SO}_3^{2-}]_0 = 0.0050 \text{ M}$, $[\text{HSO}_3^-]_0 = 0.0500 \text{ M}$ and we changed $[\text{OA}]_0$ from 0 M to 0.0100 M .

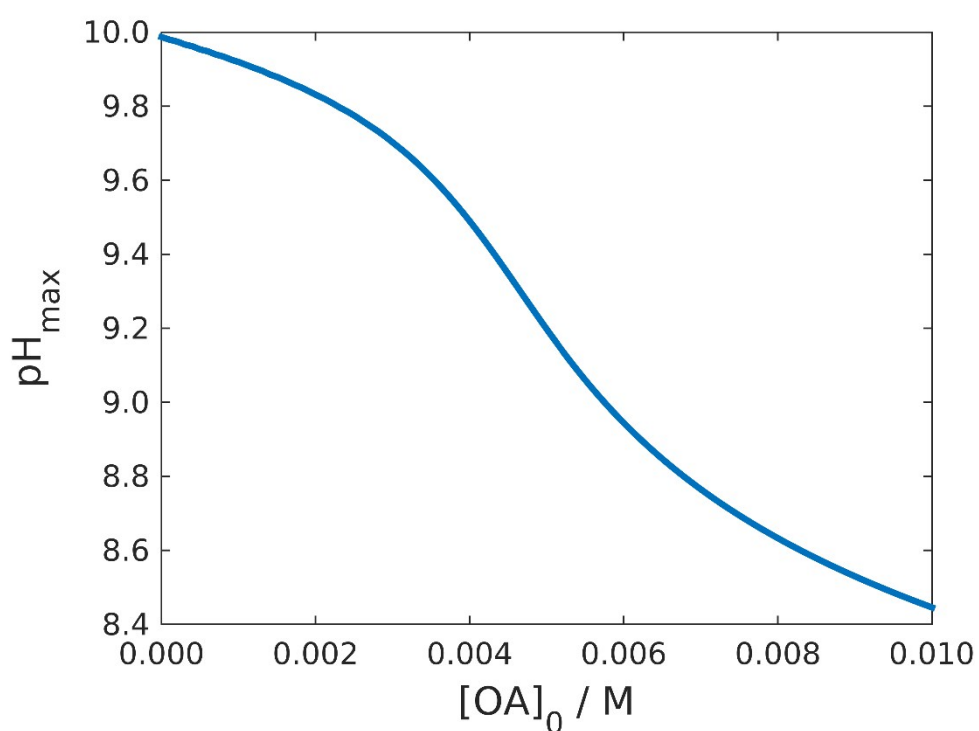


Figure S10 The calculated pH maximum in the function of the initial oleic acid concentration. The fixed initial concentrations: $[\text{CH}_2(\text{OH})_2]_0 = 0.2000 \text{ M}$, $[\text{GL}]_0 = 0.0100 \text{ M}$, $[\text{SO}_3^{2-}]_0 = 0.0050 \text{ M}$, $[\text{HSO}_3^-]_0 = 0.0500 \text{ M}$ and we changed $[\text{OA}]_0$ from 0 M to 0.0100 M.

Movies

File: Video_S1.avi

Title: (Reversible) rearrangement in the supramolecular structure of self-assembled fatty acid molecules

Legend: Time programmed and precoded vesicle-micelle-vesicle rearrangement/restructuring of oleic acid molecules in the MGS and GL system at two different initial concentrations of methylene glycol. $[\text{CH}_2(\text{OH})_2]_0 = 0.2000 \text{ M}$ (left), $[\text{CH}_2(\text{OH})_2]_0 = 0.1125 \text{ M}$ (right), $[\text{SO}_3^{2-}]_0 = 0.0050 \text{ M}$, $[\text{HSO}_3^-]_0 = 0.0500 \text{ M}$, $[\text{GL}]_0 = 0.0100 \text{ M}$, $[\text{OA}]_0 = 0.00125 \text{ M}$.

Field view: 10.4 cm \times 6.4 cm, time span: 420 s, acceleration rate: 20.

File: Video_S2.avi

Title: (Reversible) dispersion and self-assembly of AuNPs

Legend: Time programmed and precoded disassembling and reassembling of AuNP-aggregates in the MGS and GL system at two different initial concentrations of methylene glycol. $[\text{CH}_2(\text{OH})_2]_0 = 0.2000 \text{ M}$ (left), $[\text{CH}_2(\text{OH})_2]_0 = 0.1125 \text{ M}$ (right), $[\text{SO}_3^{2-}]_0 = 0.0050 \text{ M}$, $[\text{HSO}_3^-]_0 = 0.0500 \text{ M}$, $[\text{GL}]_0 = 0.0100 \text{ M}$ and the concentration of the carboxyl group attached to the nanoparticles was $3.53 \times 10^{-5} \text{ M}$.

Field view: 10.8 cm \times 6.4 cm, time span: 498 s, acceleration rate: 20.

File: Video_S3.avi

Title: Pulling and releasing (lifting and lowering) of a mechanical load by a pH-responsive hydrogel filament

Legend: Time programmed phase-separation and rehydration of polymer chains (with associated volume and elasticity changes of the network) in the MGS and VL system. Background color is provided by Phenol Red pH-indicator. $[\text{CH}_2(\text{OH})_2]_0 = 0.1125 \text{ M}$, $[\text{SO}_3^{2-}]_0 = 0.0050 \text{ M}$, $[\text{HSO}_3^-]_0 = 0.0500 \text{ M}$ and $[\text{VL}]_0 = 0.0100 \text{ M}$. Field view: 7 mm \times 32 mm, time span: 58 min 15 s, acceleration rate: 225.

References

- 1 B. Wang, X.-D. Xu, Z.-C. Wang, S.-X. Cheng, X.-Z. Zhang and R.-X. Zhuo, *Colloids Surf. B Biointerfaces*, 2008, **64**, 34–41.
- 2 J. Horváth, I. Szalai, J. Boissonade and P. De Kepper, *Soft Matter*, 2011, **7**, 8462–8472.
- 3 J. Horváth, *J. Phys. Chem. B*, 2014, **118**, 8891–8900.
- 4 J. Horváth, *Polymer*, 2015, **79**, 243–254.
- 5 E. C. Cho, J.-W. Kim, A. Fernández-Nieves and D. A. Weitz, *Nano Lett.*, 2008, **8**, 168–172.
- 6 X. S. Wu, A. S. Hoffman and P. Yager, *J. Polym. Sci. Part Polym. Chem.*, 1992, **30**, 2121–2129.
- 7 O. Okay, *Prog. Polym. Sci.*, 2000, **25**, 711–779.
- 8 X.-Z. Zhang, Y.-Y. Yang and T.-S. Chung, *Langmuir*, 2002, **18**, 2538–2542.
- 9 X. Zhang, R. Zhuo and Y. Yang, *Biomaterials*, 2002, **23**, 1313–1318.
- 10 J. M. Swann and A. J. Ryan, *Polym. Int.*, 2009, **58**, 285–289.
- 11 K. Kovacs, R. E. McIlwaine, S. K. Scott and A. F. Taylor, *Phys. Chem. Chem. Phys.*, 2007, **9**, 3711–3716.